JOURNAL OF OPTOELECTRONICS AND ADVANCED MATERIALS Vol. 12, No. 2, February 2010, p. 193 - 198

Influence of Eu^{3+} doping on the degradation property of TiO_2 nanostructures

RUEY CHANG HSIAO[a,b,*], N. SABARI ARUL[c], D. MANGALARAJ[c], RUEY SHINE JUANG[b]
[a]*Department of Chemical Engineering and Material Engineering, Lunghwa University of Science and Technology, Taoyuan, 330, Taiwan*
[b]*Department of Chemical Engineering and Material Science, Yuan Ze University, Chung-Li, 320, Taiwan.*
[c]*Department of Nanoscience and Technology Bharathiar University, Coimbatore 641 046, India*

TiO_2 nanoparticles loaded with Eu species were prepared with the aim to enhance the photocatalytic activity and to study the activity at different irradiation conditions. TiO_2 and Eu^{3+} doped TiO_2 nanostructures were synthesized by hydrothermal method. X-ray diffraction pattern showed a decrease in crystallite size and increase in the crystallinity of the sample on doping with Eu^{3+}. A reduction in the particle size was observed from the SEM and TEM images of Eu^{3+} doped TiO_2 sample. The photocatalytic activity of the undoped and Eu^{3+}-TiO_2 nanopowders was estimated towards orange (II) sodium salt (AO7) using natural solar irradiation and UV sources 20 W, 100 W and 400 W respectively. Doping of Eu^{3+} in TiO_2 has significantly improved the photodegradation and decolorization efficiency of the obtained nanostructures.

(Received January 15, 2010; accepted February 18, 2010)

Keyword: Europium doped titanium dioxide; Degradation, Orange (II) sodium salt (AO7-dye), Optical property.

1. Introduction

The impact of the morphology on the properties of high surface area materials is a field of increasing importance for understanding, creating and improving semi conducting properties of nanomaterials for wide applications [1]. For example optical, electrical, photochemical and photo physical properties of nanomaterials are attracting considerable interest in the areas of optoelectronics, quantum computing, photo catalysis, and luminescence labeling [2-6]. Besides these properties, understanding the photocatalytic behavior of nanomaterials for environmental purifications is still under debate. Among other metal oxides, TiO_2 is a highly suitable material for photocatalyst in environmental remediation processes [7-8].

Titanium oxide nanomaterial is of great interest due to their potential use as, photocatalysis, photovoltaic, solar energy conversion, sensors, textiles, paints, cosmetics and gas sensing, due to its wide band gap (3.2 eV), low cost, non-toxic nature, strong oxidizing power, high resistance to chemical or photo-induced corrosion, and maximum light scattering with virtually no absorption [9-13]. The band gap of TiO_2 lies in the near-UV of the electromagnetic spectrum: 3.2 eV (388 nm) and 3.0 eV (410 nm) for anatase and rutile, respectively [14]. As a consequence, only UV light is able to create electron-hole pairs and to initiate the photo catalytic processes. In a photochemical application, TiO_2 photocatalysis is invariably affected by the surface properties of the TiO_2 particle. Anpo et al. [15] observed a blue shift and increase in reaction yield and photocatalytic activity as the diameter of the TiO_2 particles become smaller, especially below 10 nm. This observation was attributed to the suppression of radiation less transfer and the concurrent enhancement of the activities of the charge carriers. Recently so many researchers have concentrated to improve the activity of photo catalytic and successfully synthesize of titanate and titania-based materials, including of nanorods, nanotubes, nanobells, nanosheets, nanowires, and nanoneedles [16-18]. Compared to bulk and thin film, the nanostructures show enhanced properties of photocatalysis due to smaller band gap

Furthermore many researchers concentrated on doping of rare-earth-metal compounds with TiO_2 to improve the photo activity and photoluminescence of nanostructure TiO_2 [19 -21]. Especially europium is found to be the suitable material for doping to improve those properties .The doping of the europium ions into TiO_2 creates temporary traps for the photo generated charge carriers and the enhances inhibition of their recombination during migration from inside of the material to the surface. Yibing Xie et.al reported europium ion modified TiO_2 by sol gel method to study the photo catalysis activity [22]. Shuo Li et.al reported preparation of Eu^{2+}, Dy^{3+} doped TiO_2 by sol–gel method [23]. Yuhong Zhang et.al reported Eu (0.25 to 10 atm. %) doped nanocrystalline titania by a special sol–gel method. The XRD results show that the temperature of anatase-to-rutile phase transformation is substantially increased by europium doping and the increase is not proportional to the doped lanthanide content [24]. Lucas Alonso Rocha et.al reported incorporation of europium into titanium dioxide by sol-gel method and explained the luminescence of Eu (III) ions in titanium dioxide [25]. Florin Vasiliu et.al explained photocatalytical activity of Fe- and Eu-doped TiO_2

strongly depended on its bulk and surface properties [26]. Diamandescua et.al reported the synthesis of europium-doped TiO_2 nanoparticles powders by hydrothermal method [27]. Thus eventhough a number of reports are available on the preparation of Eu doped TiO_2 by sol-gel method, not many are available on the synthesis and photocatalytic study of nanostructured europium doped TiO_2 by hydrothermal method. The present work aims at a study on the structural characterization and photo catalytic activity of undoped and doped Eu^{3+} doped TiO_2. Also we have used AO7 dye for the photocatalytic activity studies and found that this dye is having more photocatalytic activity than other reported dyes.

2. Experimental techniques

TiO_2 and Eu-doped TiO_2 were prepared by hydrothermal route. Initially, pure TiO_2 nanoparticles were prepared by hydrothermal treatment of commercially obtained TiO_2 (Merck) powder. For preparing Eu doped TiO_2, the starting precursor was commercially obtained titanium dioxide (TiO_2) powders and europium nitrate $Eu(NO_3)_3$. 2 gm of TiO_2 (Merck) was dissolved in 15 ml of DDW and 2 g of $Eu(NO_3)_3$ was dissolved in 5 ml of DDW. Both solutions were mixed well using magnetic stirrer. To the reaction mixture, 28 % aqueous ammonia was added and the pH value was adjusted to ~11. The solution was then transferred into stainless steel autoclave and maintained at 150 °C for 24 hours. After that the precipitate was washed with ethanol and DDW. The precipitate was dried at 80 ^oC for 24 h. The as-obtained products were used for further characterization. The photo catalytic activity of the prepared samples was assessed by the degradation experiment towards 30 ppm aqueous solution of orange (II) sodium salt (AO7, Sigma Co).

2.1 Characterization

The prepared samples were structurally characterized by using X-ray diffraction (XRD) analysis using a Cu-Kα_1 radiation (RIGAKU X- RAY DIFFRACTOMETER D/MAX-2200). The morphology, particle size and size distribution of particles were investigated by a Field Emission Scanning Electron Microscope (FESEM JEOL JSM-6500) at 10 kV after sputtering coating platinum for conduction. To gain further insight into the microstructures, Transmission Electron Microscopic (TEM) investigations were performed using a JEOL JEM-2100. Samples for TEM analysis were prepared by air-drying a drop of a sonicated suspension of the dried precipitate in ethanol onto copper grids. The photocatalytic degradation efficiency of the prepared samples was assessed by the degradation of 30 ppm aqueous solution of AO7 under natural solar radiation and ultraviolet irradiations with sources having power of 20, 100 and 400 W. The absorbance of AO7, after different durations of irradiation was observed by measuring the transmittance spectra using a JASCO V-670 UV-Vis spectrometer. The photocatalytic experiments were carried out in a batch photo reactor consisted of a borosilicate glass vessel (800 cm^3) mounted suitably on a magnetic stirrer.

3. Results and discussion

3.1 X ray diffraction analysis

Primary structural information was obtained from the XRD patterns of the hydrothermally prepared samples. The XRD pattern (Fig.1a) of the hydrothermally treated commercial TiO_2 sample revealed the presence of both anatase and rutile TiO_2 phases. Eu doped TiO_2 sample (Fig 1b) has more anatase phase and less rutile phase, and no new crystal phases are produced by doping. The XRD pattern shows that the Eu–TiO_2 powder samples have peaks at 2θ = 25.4°, 37.8°, 48.2°, 54.6°, and 63.0° which are corresponding to that of anatase titania [28]. It can be seen from the Fig.1 that the XRD peaks shifted to lower diffraction angle with the doping of Eu into TiO_2. This may be due to the inclusion of Eu into the TiO_2 lattice which shifts the peak towards the lower angle region. Fig. 1(inset) displays the enlarged XRD peaks of anatase TiO_2 plane (1 0 1) in the 2θ region of 24.0–26.01.

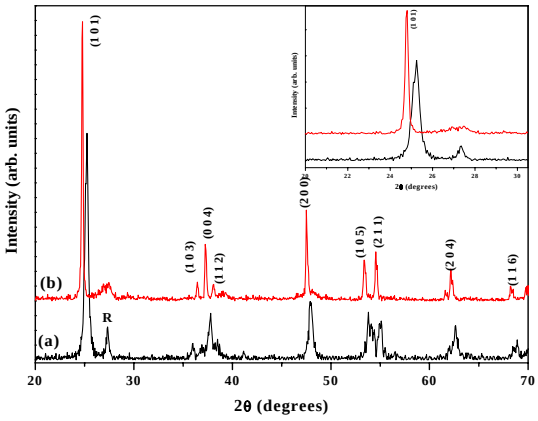

Fig. 1. XRD patterns of (a) pure and (b) Eu doped TiO_2. Inset: Enlarged portion of [101] plane shows the shift after the addition of Eu.

It can be found that the XRD peaks of crystal plane A (1 0 1) shifts to lower diffraction angle when Eu is doped into TiO_2. Scherrer' formula was used to calculate the average crystallite size of the nanoparticles.

For pure TiO_2, the average crystallite size was to be around 15 nm, and for Eu doped TiO_2 it was around 8 nm. A change in the intensity of the XRD pattern could also be observed along with the peak shift and the change in

average crystallite size. The peak intensity increased significantly due to the addition of Eu. Hence it can be concluded that the addition of the Eu influenced the structural properties and the crystallinity of the product. The calculated lattice constants for pure TiO_2 were in agreement with the corresponding values (a = 0.3782 nm and c = 0.952 nm) as reported by Okada et al. [29].

3.2 Field Emission Scanning Electron Microscope

The field-emission scanning electron microscopy (FE-SEM) was used to observe the changes in morphological features of TiO_2 before and after Eu doping. Figure 2 a, b shows the FESEM images of the pure and Eu doped TiO_2 respectively. It can be seen that the crystallite size is reduced with the addition of Eu. This is in well accordance with the reported data [29]. The average particle size of the samples of TiO_2 and Eu/TiO_2 measured by SEM, is around 40-45 nm and 20 -25 nm respectively as shown in Fig. 2. Though the particle size has reduced significantly, the doping of Eu on TiO_2 particles has resulted in the aggregation of TiO_2 particles.

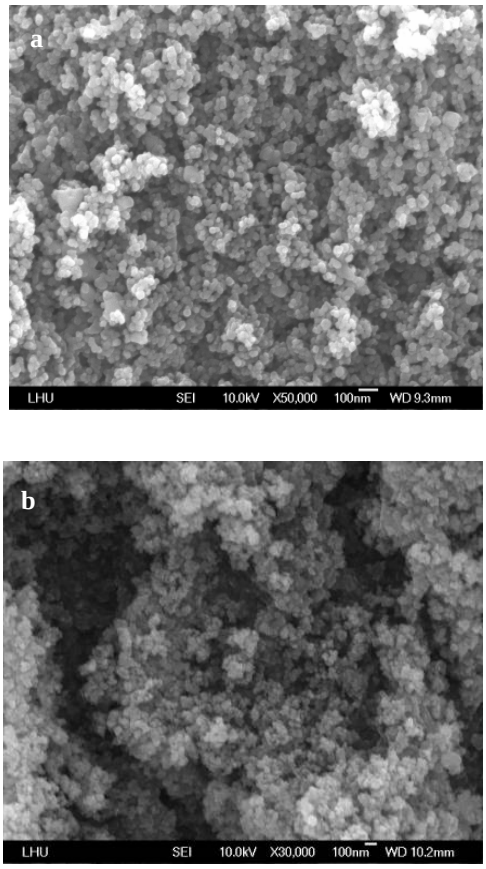

Fig. 2. FESEM images of (a) pure and (b) Eu doped TiO_2

3.3 Transmission Electron Microscopic Analysis:

To get further insight into the morphology of the product TEM analysis was carried out. Fig. 3 shows the TEM images of the pure and Eu doped TiO_2. The results are in well agreement with the obtained SEM analysis. The mean particle size of the pure TiO_2 is around 40 nm and for Eu doped TiO_2, the particle size is about 20 nm. It is seen that a rectangular and quadratic morphology are predominant for undoped and Eu-doped TiO_2 samples (Fig. 3a).

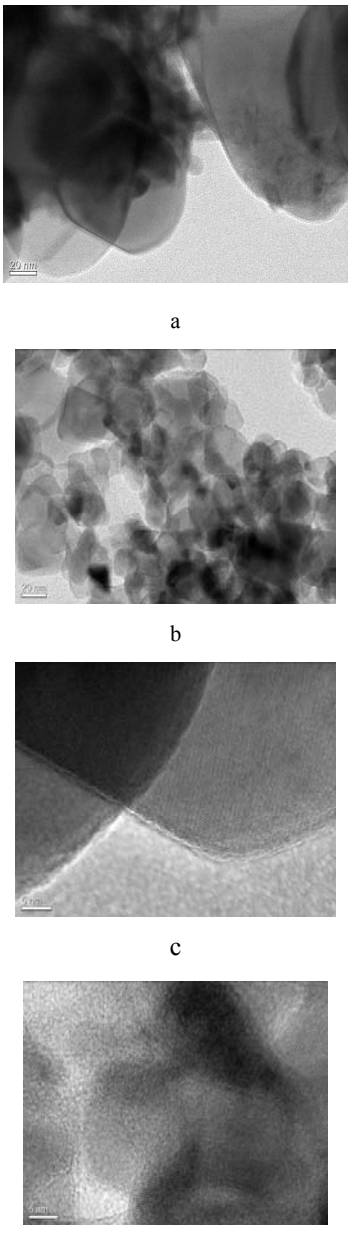

Fig. 3. TEM and HRTEM images of (a,c) pure and (b,d) Eu doped TiO_2 respectively.

In the case of Eu-doping in TiO_2, the particle size is reduced significantly as can be seen clearly in Fig. 3. Also the size distribution is almost uniform everywhere. The interplanar distances measured in HRTEM lattice image of Eu doped sample (Fig. 3c,d) were ~0.352 nm, corresponding to the interplanar spacing of the [101] plane of the anatase TiO_2.

3.4 Raman analysis

The Raman spectra for TiO_2 and Eu doped TiO_2 nanocrystals are shown in Fig. 4. It shows the Raman peaks at 141, 393, 514 and 634 cm^{-1} that can be assigned to the Eg, B1g, A1g and Eg modes of the anatase phase, respectively. By comparing the Raman spectra of the TiO_2 nanocrystal with that of bulk TiO_2, it can be seen that the spectral change is related to the oxygen stoichiometry, surface pressure and phonon confinement

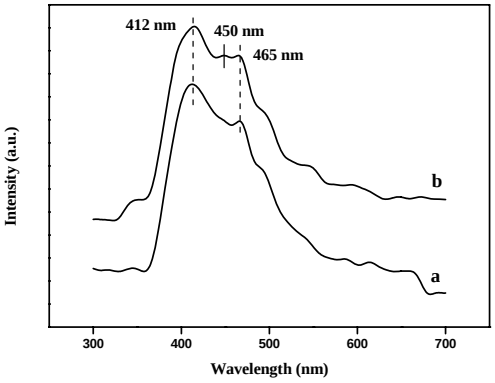

Fig. 4. Raman spectra of (a) pure and (b) Eu doped TiO_2

effect. A similar phenomenon has also been observed previously [30]. Low concentration of Eu doping does not modify the nanocrystalline modes in TiO_2.

3.5 Photoluminescence analysis

Fig. 5 shows the PL emission spectra for TiO_2 and Eu doped TiO_2 samples excited by a wavelength of 275 nm. The emission spectra of the as-prepared TiO_2 have two main characteristic peaks centered at 412 and 465 nm which are in the blue emission region with that of bulk TiO_2 [31].

This emission spectrum confirms that the as-prepared TiO_2 samples are in the nano-range of size distribution. It has been previously reported that the emission peak at 412 nm is from the free exciton in rutile TiO_2 phase [31]. Similarly, Eu doped TiO_2 sample have three characteristic peaks at 412, 450 and 465 nm.

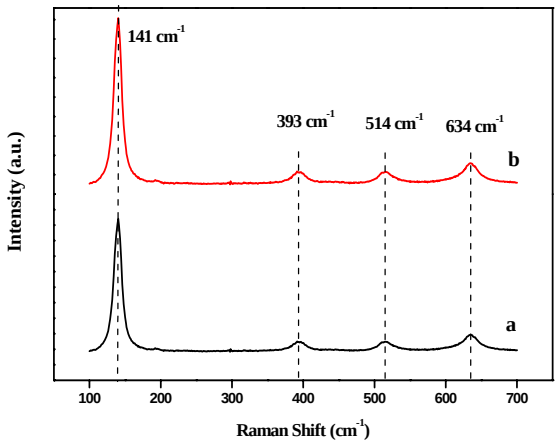

Fig. 5. PL spectra of (a) pure and (b) Eu doped TiO_2

In addition, the normalized intensity of the peaks at 412 and 465 nm is intensified with the increase of Eu content in Eu doped TiO_2 nanocrystals. These suggest that the two emission peaks at 412 and 465 nm originate from different luminescent centers. In Eu doped TiO_2 nanocrystal samples, the formation of the Eu–O–Ti bonds may act as defects or impurity centers on the surface of the TiO_2 crystallite, in which the exciton can be trapped and recombination happens [31]. Additionally, the XRD result complements the PL emission spectra, showing that rutile content in the sample decreases with the increase in Eu content; thus, the normalized intensity peaks at 412 and 465 nm are intensified. The peak at 450 nm may be due to the increase in the defect centre of TiO_2 nanocrystals due to the doping of Eu^{3+} ions.

3.6 Photocatalytic activity

The photocatalytic activity of the prepared samples was estimated under five different conditions, namely, (1) without catalyst, (2) with catalyst (commercial Titanium dioxide) under solar illumination (3) with catalyst (commercial Titanium dioxide) under UV illumination from 3 different sources (4) with catalyst (Eu doped TiO_2) under solar illumination (5) with catalyst (Eu doped TiO_2) under UV illumination from 3 different sources. The absorbance maximum steadily decreased on illuminating the sample under solar light and UV light. This marks the beginning of the degradation activity by the catalyst. Photocatalytic activity of the prepared samples was carried out using the UV lamp of power 20, 100 and 400 W. Figure 6 shows the decrease of AO7 concentration under Solar and UV irradiation in the presence of TiO_2 and Eu doped TiO_2 samples.

The decolourisation efficiency and the degradation rate constant were determined using the formula,

$$\frac{C_0 - C}{C_0} \times 100 \quad (1)$$

where, C_0 is the initial concentration or the concentration at t = 0, C is the concentration of the dye after complete degradation. The decolourization efficiency of pure and Eu doped TiO_2 is shown in Table 1.

In addition to that, the apparent rate constant of photocatalytic degradation of AO7 was calculated from the expression,

$$\ln\left(\frac{C_0}{C_t}\right) = kt \quad (2)$$

Where k is the rate constant of the reaction, C_o, C_t are the concentration of the dye at t=0 and after complete degradation respectively. The apparent rate constant was determined from the slope of the plot between Co/C_t and irradiation time.

Table 1. Kinetic rate constant and decololourization efficiency of pure and Eu doped TiO_2 for different irradiation sources.

Irradiation source	Samples	K (1/Min)	D.E. (80min.)
Solar	TiO_2	0.02678	0.63
	Eu doped TiO_2	0.00243	0.16
UV 20W	TiO_2	0.00727	0.43
	Eu doped TiO_2	0.007024	0.37
UV 100W	TiO_2	0.03009	0.91
	Eu doped TiO_2	0.0914	0.96
UV 400W	TiO_2	0.06047	0.93
	Eu doped TiO_2	0.0801	0.99

From the Table 1 it can be observed that, the degradation activity was higher in the case Eu doped TiO_2 sample. This confirms that, doping of Eu^{3+} enhances the photocatalytic activity of TiO_2.

Kinetic rate constant (k) and decolourization efficiency (DE) of the Eu doped sample TiO_2 with different irradiation sources is shown in figure 6. Compared to all other irradiation sources, 20 W UV has the lower value for both k and DE. The solar irradiation shows the better rate constant than 20 W UV source. But when the power of the irradiation source is increased further to 100 and 400 W, there is a significant increase in the k which is clearly deduced from the figure 6. Similarly for the DE, 20 W shows the lower value compared to solar irradiation and after increasing the irradiation power, there is a considerable increase in the DE value. For different photocatalysts, the decolourization efficiency follows the order 20 W UV source < Solar irradiation < 100 W UV source < 400 W UV source

4. Conclusions

TiO_2 and Eu doped TiO_2 nanoparticles are prepared by hydrothermal method. XRD patterns reveal the anatase phase in hydrothermally synthesized samples. The mean grain size was less than 15nm and the morphology was found to depend on doping element. The Eu doped TiO_2 significantly reduced the grain size. Photoluminescence spectra confirm that in Eu doped TiO_2 samples the formation of the Eu–O–Ti bonds may act as defects or impurity centers on the surface of the TiO_2 crystallite, in which the exciton can be trapped and recombination happens. Blue shift occurs in Eu doped TiO_2 nanoparticle. The photocatalytic activity of the synthesized samples was carried out using AO7 dye with different irradiation sources and the obtained results shows that Eu doped TiO_2 for 400 W UV irradiation source were better than the other sources.

Acknowledgement

One of the authors (R.C. Hsiao) would like to thank Prof. Kuen Ting (Former Dean), Prof. Pao Chi Chen (Dean), Dr. Hsiu Ling Hsu (Asso. Prof.) and Dr. Rosilda Selvin (Asst. Prof.), Department of Chemical Engineering and Material Engineering, Lunghwa University of Science and Technology for their help and encouragement. He expresses his thanks to the research scholars of Bharathiar University, Coimbatore, India for their kind support and help towards this work. He is also indebted to his project student, Mr. Chuan qui Huang, for his kind cooperation to carry out this work.

References

[1] D. Wang, R.Yu, Y. Chen, N. Kumada, N. Kinomura, M.Takano, Solid State Ionics. **172,** 101-104(2004).
[2] K. Ando, Solid State Sci. **128**, 211(2000).
[3] M. Shim, C. Wang, D. J. Norris, P. Guyot-Sionnest, MRS Bull. **26**, 1005 (2001)
[4] V. N. Golovach, D. Loss, Semicond. Sci. Technol. **17**, 355(2000)
[5] Z. Zou, J.Ye, K. Sayama, H.Arakawa, Nature. **414**, 625(2001)
[6] W. C. Chan, S. Nie, Science, M. Bruchez, M. Moronne, P.Gin, S.Weiss, A.P. Alivisatos, Science, **281**, 2013 (1998)
[7] J. C. Colmenares, R. Luque, J.M. Campelo, F. Colmenares, Z. Karpiñski, A. Angel, Romer Materials, **2**, 2228 (2009)
[8] H. Kim, S.Lee, Y. Han, J. Park, J. Mater. Sci. **40**, 5295 (2005).

[9] M. Ferrara, Nanostruct. Mater. **7,** 709 (1996).
[10] H. Tang, Sens. Actuators B **26**, 71 (1995).
[11] D.C. Gilmer, Chem. Vapor. Depos. **4**, 9 (1998).
[12] K. Bange, C.R. Otterrnann, O. Anderson, U. Jeschkowski, M. Laube, R. Feile, Thin Solid Films **197,** 279 (1991).
[13] Y. Sawada, Y. Taga, Thin Solid Films **116 ,** 155(1984).
[14] R. Isono, T. Yoshimura, and K. Esumi, J Colloid Interface Sci, **2881**, 177(2005)
[15] M. Anpo, T. Shima, S. Kodama, Kubokawa, J. Phys. Chem. **91**, 4305 (1987).
[16] Y. X. Zhang, G. H. Li, Y. X. Jin, Y. Zhang, J. Zhang, Chem. Phys. Lett. **365**, 300-4(2002).
[17] P. D.Cozzoli, A. Kornowski, H. J. Weller, J. Am. Chem. Soc. **125**, 14539 (2003).
[18] Z. R. R. Tian, J. A. Voigt, J. Liu, B. McKenzie, H. Xu, H. F. Large, J. Am. Chem. Soc. **125**, 12384 (2003).
[19] W. Choi, A. Termin, M. R. Hoffmann, Angew. Chem. 106, 1148(1994).
[20] W. Choi, A. Termin, M. R. Hoffmann, Angew. Chem. Int. Ed. Engl. **33**, 1091 (1994).
[21] T. Lopez, J. Hernandez-Ventura, R. Gomez, F. Tzompantzi, E. Sanchez, X. Bokhimi, A. Garcya, J. Mol. Catal. A: Chem. **167**, 101(2001).
[22] Y. Xie, C. Yuan, Mater. Res. Bull. **39**, 533 (2004).
[23] S. Li, W. Wang, Y. Chen, L. Zhang, J. Guo, M. Gong, Catal. Comm. **10**, 1048 (2009).
[24] Y. Zhang, H. Zhang, Y. Xu, Y. Wang, Materials Research, **8**(3), 361 (2005)
[25] L. A. Rocha, L. R. Avila, B. L. Caetano, E. F. Molina, H. C. Sacco, K. J. Ciuffi, P. S. Calefi, E. J. Nassar, J. Mater. Chem.**13**, 2261 (2003)
[26] L. Florin Vasiliu, E. D. Diamandescu, D. Macovei, C. M. Teodorescu, D. Tarabasanu-Mihaila, A. M. Vlaicu, V. Parvulescu, Top Catal. **52**, 544 (2009).
[27] L. Diamandescua,., F. Vasiliu, D. Tarabasanu-Mihaila, M. Federa, A. M. Vlaicua, C. M. Teodorescua, D. Macovei, I. Enculescua, V. Parvulescub, E. Vasilec Journal of Mater Chem and Phys. **112,** 146 (2008).
[28] Yibing Xie, Chunwei Yuan, Mater. Res. Bull. **39**, 533 (2004).
[29] Q. G. Zeng, Z. J. Ding, Z. M. Zhang, J. Lumin, **118,** 301 (2006).
[30] K. Okada, N. Yamamoto, Y. Kameshima, A. Yasumori, K. J. D. MacKenzie, J. Am. Ceram. Soc. **84**, 1591(2001).
[31] L. G. J. Haart, G. Blasse, J. Solid State Chem. **61**, 135(1986).

*Corresponding author: hrc@mail.lhu.edu.tw